Solving the Optimal Mistuning Problem by Symmetry: A General Framework for Extending Flutter Boundaries in Turbomachines via Mistuning

Benjamin Shapiro
bshapiro@indra.caltech.edu

Technical Report: 97-004
Control & Dynamical Systems
California Institute of Technology
Pasadena, California 91125

Abstract

A general framework is presented for analyzing and optimizing stability increases due to mistuning. The framework given is model independent and is based primarily on symmetry arguments. Difficult practical issues are transformed to tractable mathematical questions. It is shown that mistuning analysis reduces to a block circular matrix eigenvalue/vector problem which can be solved efficiently even for large problems. Similarly, the optimization becomes a standard linear constraint quadratic programming problem and can be solved numerically. Since the methods given are model independent, they can be applied to various models and allow the researcher to easily conclude which models accurately capture mistuning, and which do not. A simple quasi-steady model for flutter in a cascade is used to illustrate and validate results in this paper.

1 Introduction

Jet engine performance is severely limited by a wide variety of instabilities including inlet buzz, shear layer turbulence and compression instabilities (see Figure 1). The ability to eliminate or reduce

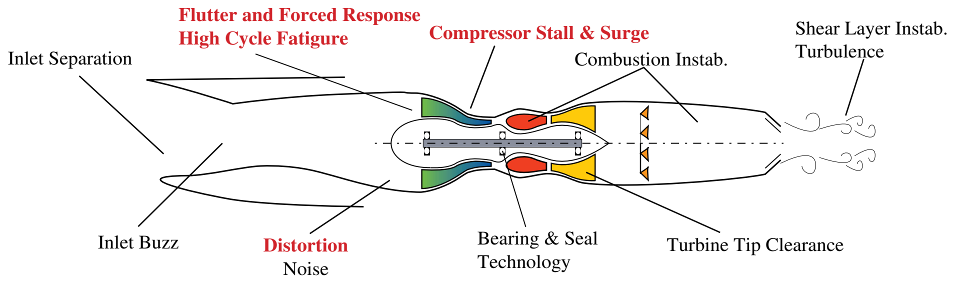

Figure 1: Turbomachinery instabilities. (Figure courtesy J. Paduano)

the severity of these instabilities can lead to increased safety, higher efficiency and significant cost and weight savings in future engine designs. This work focuses on flutter in compression systems since it is encountered in every regime of engine operation and clearly limits engine performance (see Figure 2). The interested reader is referred to [9] for a general overview of turbomachinery instabilities.

In this paper we study passive control of flutter using mistuning. In this context, mistuning refers to symmetry breaking. For example, all the blades in a spinning fan or bladed disc are nominally identical and so there exists a discrete circumferential symmetry. It has been noted numerically [2, 5, 10] and experimentally [19] that if we *mistune* these blades by making them different from one another, then the flutter boundary can be delayed dramatically. Techniques presented herein restrict attention to circumferential symmetry breaking but apply to any type of instability. We use flutter in compression systems as a concrete example and note that the same methods hold for other instabilities such as rotating stall or surge.

Experiments have shown that mistuning rotor stiffness in compression systems not only increases the range of stability but also creates undesirable "side effects" such as mode localization [7, 8, 20] and decreased operating range [17]. This leads to two natural questions:

1 *Analysis: For a given mistuning find new stability boundaries and resulting "side effects".*

2 *Synthesis: When is mistuning beneficial? If it is, find* optimal *mistuning (increase stability with acceptable "side effects").*

Variations on the analysis issue have been addressed in past research. Dugundi and Bundas [6] use Whitehead's aerodynamic coefficients [18] to predict the stability increase for alternate blade mistuning. Bloemhof [4] considers stability increases due to single, double and triple blade alternate mistuning along with aperiodic or random mistuning. As regards the second part of the analysis question, we note that most work on predicting "side effects" as a function of mistuning has focused on mode localization. Papers in this area include [6, 10, 15, 16, 20]. Work on related "side effects" such as decreased operating range can be found in Srinivasan and Frye [17]. However, efficient solutions to the synthesis issue do not exist at this time mainly because there are no efficient solutions of the analysis problem for *arbitrary* mistuning. Crawley, Hall [5] and Nissim, Haftka [14] tackle an optimization problem where they minimize the size of mistuning (implicitly assuming that resulting "side effects" are also minimized) subject to a required stability increase. Even though

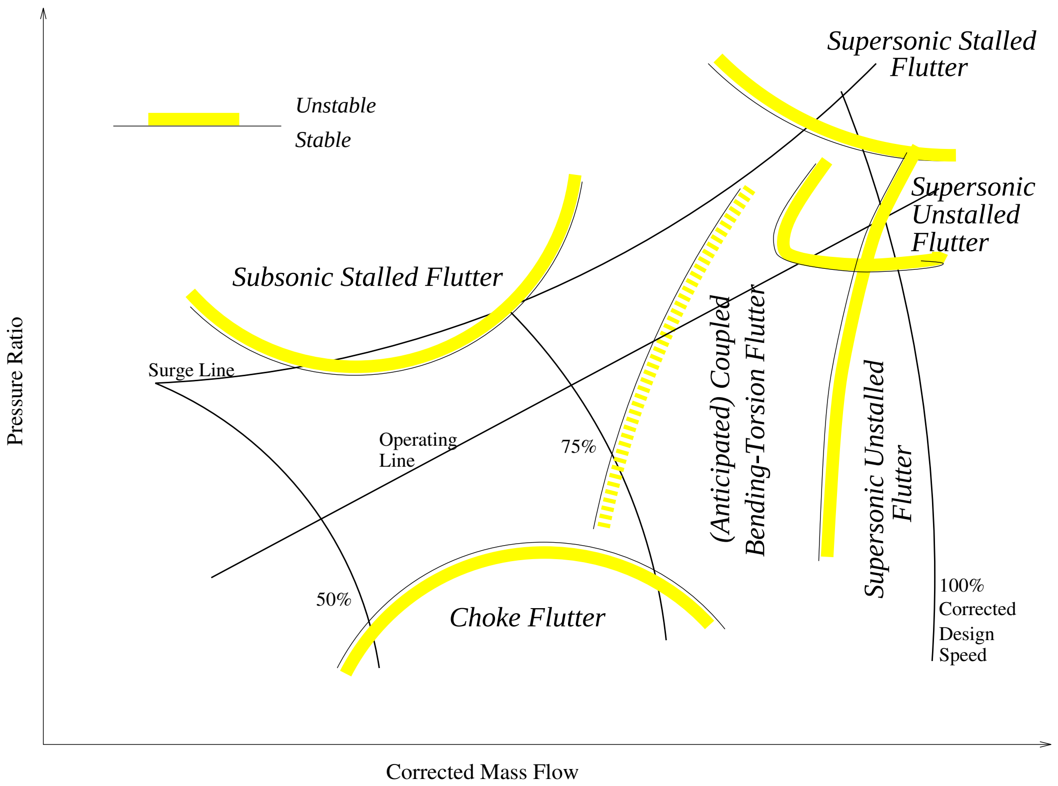

Figure 2: Compressor map showing typical flutter boundaries [3].

this is a reasonable approach, we note that in both papers only local optimums are found and both methods are restricted to small problems (less then 14 blades) by lengthy computation times.

Furthermore, previous mistuning work has not made use of symmetry arguments to aid in the analysis. Yet mistuning is concerned primarily with symmetry and symmetry breaking and so symmetry arguments form the natural tools for the mistuning problem. Using simple symmetry arguments which apply to *any* model type—be it computational fluid dynamic (CFD), sinusoidal imposed motion, or dynamical system—simplifies the analysis problem tremendously. Finding the stability boundary as a function of *arbitrary* mistuning reduces to finding $r/2+2$ stability coefficients where r is the number of blades. One then requires a specific model to evaluate the $r/2+2$ stability coefficients.

We give two methods to compute these stability coefficients. Method A (Section 4.1) is valid for any dynamical systems model of the form $\dot{x} = f(x)$ and method B (Section 4.2) is practical for CFD models of small to moderate size. Method A relates the stability coefficients to a block circular matrix eigenvalue/vector problem which can be solved efficiently even for large problems while method B involves the finite difference of CFD stability results. Future research could lead to further methods which would compute the stability coefficients for large CFD codes and imposed sinusoidal motion models.

Our focus is on dynamical system models as opposed to imposed sinusoidal motion models because it is more natural to study mistuning in the former case. In particular, imposed motion models usually assume constant inter-blade phase angle. Although this assumption is valid in the tuned case, upon mistuning the eigenvectors (which correspond to the imposed motion) are perturbed away from the symmetric case and so the constant inter-blade phase angle assumption is violated. Our analysis of unconstrained dynamical system models avoids these difficulties.

We note that the same *model independent* symmetry arguments used in the analysis can be used to reduce the optimization problem to a standard quadratic programming problem with constraints. In this paper we simply restrict the maximal size of allowable mistuning and assume that resulting "side effects" are acceptable. Consequently, the optimization becomes a linear constraint quadratic program. Using branch and bound software developed by Faiz et al [1] it is possible to find global optimums for fairly large problems (up to about thirty blades). More realistic constraints motivated by "side effects" in general and mode localization in particular shall be addressed in future research. Finally, to further illustrate the power of symmetry arguments we show that with additional structure found in the quasi-steady model of Appendix (A), the (different) optimal arrangement problem of Section 6 may be solved closed form.

2 Problem Setup

As motivation, consider a compressor fan with r blades. Nominally, all the blades are identical and there exists a $2\pi/r$ circumferential symmetry. Similarly, stators, struts and inlet guide vanes (IGVs) can also possess circumferential symmetries. Given such a tuned system with r discrete objects—such as blades, stators or IGVs—and a $2\pi/r$ circumferential symmetry begin by defining a mistuning vector $z \in \mathbb{R}^{\mathrm{r}}$. An element z_i denotes mistuning for the ith object. For example, if we mistune the stiffness of r rotors, then define the ith blade stiffness $k_i = k_0(1 + z_i)$ where k_0 is the nominal or tuned stiffness. In general, we will define z so that $z = 0$ corresponds to the tuned case.

Our next goal is to define the increase in stability boundary, $s(z)$, due to mistuning. To do this in a precise way consider a dynamical system model of the form

$$\dot{x} = f(x, U, z), \tag{1}$$

where $x \in \mathbb{R}^{\mathrm{n}}$ is the state vector, $U \in \mathbb{R}$ is a *loading parameter* such as throttle, mach-number, reduced frequency or rotor speed, and z is the previously defined mistuning vector. In this context, f can be any discrete blade model or even a computational fluid dynamics (CFD) model. It is stressed that although we focus on *dynamical system* models (1), the symmetry arguments presented apply more generally. These arguments are valid for any model with symmetry, symmetry breaking and a stability boundary $s(z)$. In particular the symmetry methods apply to imposed sinusoidal motion models.

For a fixed z, as we vary the loading parameter U within some operating range $[U_0, U_1]$, the system (1) traverses a set of equilibria $X_0(U, z)$ defined by

$$X_0(U, z) = \{x_0 : f(x_0, U, z) = 0, U \in [U_0, U_1]\}. \tag{2}$$

Assuming that $X_0(U, z)$ is non-empty for z in some neighbourhood of the origin and for all $U \in [U_0, U_1]$, we pick a subset $x_0(U, z) \subset X_0(U, z)$ which corresponds to the equilibrium point of interest at each U. As an example, suppose we have a model (1) of a (tuned) jet engine with $z = 0$, U is the throttle and it varies between U_0 and U_1, then we can think of $x_0(U, 0)$ as the design operating point which varies as a function of throttle setting. Clearly, $x_0 : \mathbb{R} \times \mathbb{R}^{\mathrm{r}} \to \mathbb{R}^{\mathrm{n}}$ is a function of U and z, possibly discontinuous and non-smooth in both arguments. Continuity and smoothness assumptions for $x_0(U, z)$ will be discussed in the next section. It is important to realize that the z dependence in $x_0(U, z)$ is essential. Consider once again stiffness mistuning: since different blades have different stiffnesses, their nominal (or static) deflections are no longer equal which implies that the mistuned equilibrium point is not equal to the tuned equilibrium point ($x_0(U, z) \neq x_0(U, 0)$ for $z \neq 0$).

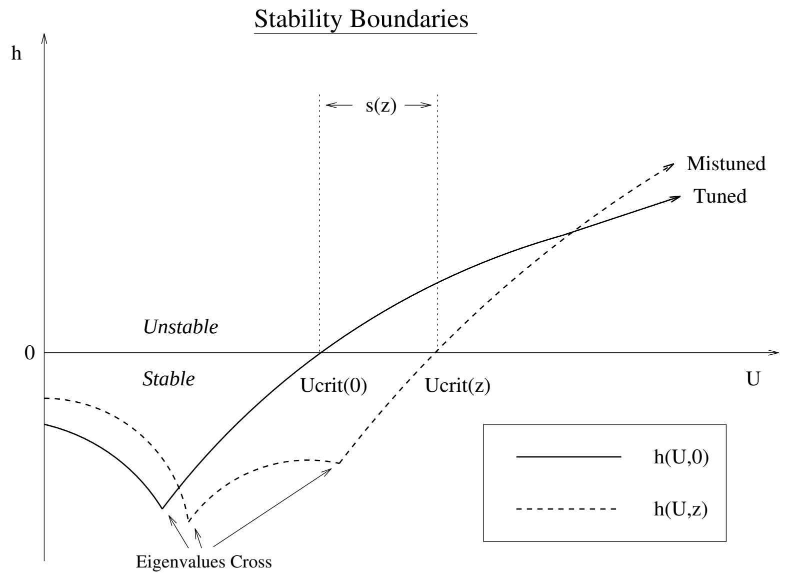

Figure 3: Increase in stability boundary, $s(z)$.

Now consider the stability of $x_0(U, z)$ as a function of U for a fixed z. Define

$$h(U, z) = \max[\mathrm{Re}(\lambda(U, z))], \tag{3}$$

where $\lambda(U, z)$ are the eigenvalues of $\frac{\partial f}{\partial x}(x_0(U, z), U, z)$. If $h(U, z)$ is negative (resp. positive) then the equilibrium point $x_0(U, z)$ is stable (resp. unstable). Since we are concerned with stability, it is assumed that as the loading U increases, then at some point U_{crit} stability is lost. Thus, define

$$U_{crit}(z) = \min_{u \in [U_0, U_1]} \{u : h(u, z) = 0\}. \tag{4}$$

If $h(U, z)$ does not cross the origin for $U \in [U_0, U_1]$ then let $U_{crit}(z) = \pm\infty$ with appropriate choice of sign. (When the system loses stability as U decreases the min should be replaced with a max. Also, if there is more then one stability boundary of interest, the interval $[U_0, U_1]$ may be appropriately partitioned so that only one boundary is under consideration.) Finally, the increase in stability $s(z)$ is defined as

$$s(z) = +[U_{crit}(z) - U_{crit}(0)] \tag{5}$$

where the positive sign is replaced with a negative if instability occurs as U decreases.

To summarize, $s(z)$ is simply the change in stability (at the relevant equilibrium point) as a function of mistuning. The technical remarks above are appropriate because they allow us to equate assumptions on the smoothness of s with smoothness conditions on f. For a graphical interpretation see Figure 3.

3 Assumptions

Two basic assumptions are required for the analysis that follows.

Assumption 1 (Smoothness) *The stability extension $s(z)$ is three times differentiable in some sufficiently large neighbourhood of the origin, $s \in C^3(\Omega)$.*

Smoothness is necessary so that we may take derivatives with respect to z. We also require that the analysis holds in some sufficiently large region Ω about the origin (tuned case) so that predicted shifts in stability hold for a physically practical range of mistuning values z. Note that Assumption 1 is a technical condition which can be relaxed in a more detailed, but equally straightforward, analysis. Such an extension typically requires the tracking of multiple eigenvalues.

Assumption 1 is easy to check if system (1) is simple. As a concrete example, Assumption 1 can be verified for the quasi-steady model used later in this paper. More generally, some fairly weak assumptions (which may be difficult to check) on the original model $\dot{x} = f(x, U, z)$ imply Assumption 1. We briefly mention three cases that can violate Assumption 1.

Case one occurs if the equilibrium point $x_0(U, z)$ does not travel smoothly with U and/or z. Typically, such problems are caused by equilibrium bifurcations and present a host of difficulties which must be dealt with before stability can be considered. Case two comes about if $h(U, 0)$ has a degenerate root at $U_{crit}(0)$ as shown in Figure 4.

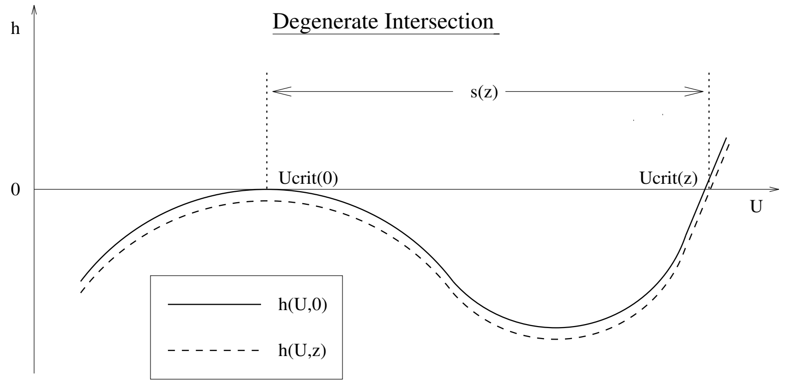

Figure 4: Discontinuous Increase in Stability Boundry.

Here $s(z)$ is discontinuous in z and Assumption 1 is violated. Under such circumstances one would consider the minimum damping instead of the stability extension $s(z)$. Case three illustrates a possible restriction on the second part of Assumption 1. If the real part of the least stable (or critical eigenvalue) in $h(U, 0)$ is very close to the real part of another eigenvalue, then it is possible that these real parts will switch as z is varied (see Figure 5).

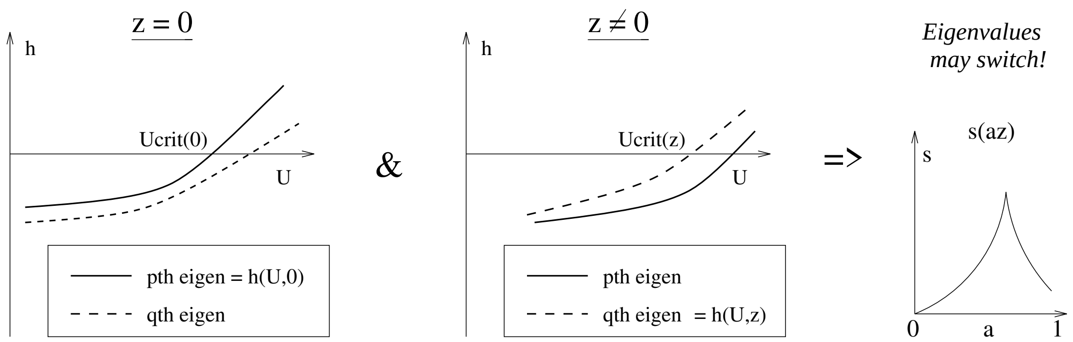

Figure 5: Eigenvalue switching creates a discontinuity in $s(z)$.

In this case $s(z)$ will be smooth on a very small region and the second part of Assumption 1 is broken. For a non-distinct least stable eigenvalue we have the special case where $s(z)$ can be discontinuous at the origin. It is possible to avoid these problems by keeping track of a number of eigenvalues during the analysis.

Assumption 2 captures the symmetry of the problem and is the main driving force behind the analysis.

Assumption 2 (Symmetry) *The minimum damping $h(U, z)$, and hence the stability extension $s(z)$, are invariant under rotations of z. Specifically,*

$$h(U, z) = h(U, \varphi^k[z]), \quad \forall U, z, \quad \forall k \in (1, 2, \dots, r-1) \tag{6}$$

$$\Rightarrow \quad s(z) = s(\varphi^k[z]), \quad \forall z, \quad \forall k \in (1, 2, \dots, r-1) \tag{7}$$

where $\varphi^k[z_1, z_2, \dots, z_r] = [z_{1+k}, z_{2+k}, \dots, z_r, z_1, \dots, z_k]$ is the rotation operator

This is the symmetry group discussed in the introduction and problem setup. In physical terms: the system should exhibit identical behaviour if we mistune the ith (say first) or jth (say third) blade (object). Specifically, the stability boundary must remain the same, hence $s(\epsilon, 0, \dots, 0) = s(0, 0, \epsilon, 0, \dots, 0)$. Alternatively, a rotation of z corresponds to a circular renumbering of blades. Since labeling schemes are arbitrary it follows that stability cannot be changed by such renumbering and so $s(z)$ is invariant under rotation. In spite of its simplicity, Assumption 2 will yield a surprising amount of analytical mileage.

Of course "perfect tuned fans" do not exist in practice and so strictly speaking Assumption 2 fails. However, we may consider a practical fan as a small perturbation ε of the nominal or theoretically perfect fan. Upon applying mistuning to this realistic fan, we introduce a larger intentional perturbation ξ for a total mistuning $z = \varepsilon + \xi$. Assumption 2 now applies to z. It will be shown in the next section that mistuning appears as a second order effect (possibly with large quadratic coefficients) and so sufficiently small (zero average) imperfections ε produce negligible stability effects. The size of "sufficiently small" depends on the ratio α^* of linear to quadratic coefficients (see Section 5, eqn. (48)). Finally note that Assumption 2 holds for most practical models, in particular it holds for models in all the mistuning articles cited in this paper.

4 Analysis

In this section we address the analysis problem: given a mistuning z find the related stability extension $s(z)$. Mode localization due to mistuning will be addressed in future work. At present, we restrict the size of mistuning (as described in the next section) and assume that the resulting mode localization is acceptable.

Our goal is to determine the form of $s(z)$. By Assumption 1, we can expand $s(z)$ in a Taylor series about the origin,

$$s(z_1, \dots, z_r) = \sum_{i=1}^{r} a_i z_i + \sum_{i,j=1}^{r} b_{ij} z_i z_j + O(\|z\|^3). \tag{8}$$

The Taylor expansion holds in a region no bigger then Ω—the range where $s(z)$ is smooth. Let $\Theta \subset \Omega$ be the subset where $s(z)$ is accurately approximated by second order terms in z. It is additionally assumed that this smaller set Θ is still sufficiently large to be of practical interest. If this is not the case, the analysis can be extended to include third and fourth order terms at the expense of increased complexity and computation time.

By Assumption 2, $s(z) = s(\varphi^k[z])$ for all integers k. Pick $z = [\epsilon, 0, \dots, 0]$ and substitute $\varphi^k[z]$ into the Taylor expansion for all $k \in (0, 1, 2, \dots, r-1)$ to get

$$a_1 \epsilon + b_{11} \epsilon^2 = a_2 \epsilon + b_{22} \epsilon^2 = \dots = a_r \epsilon + b_{rr} \epsilon^2 \tag{9}$$

which holds for all ϵ up to $O(\epsilon^3)$. Consequently,

$$a_i = a_j \tag{10}$$
$$b_{ii} = b_{jj} \tag{11}$$

for all i and j. Similarly, let $z = [0, \ldots, 0, \epsilon, 0, \ldots, 0, \epsilon, 0, \ldots, 0]$ where the ϵs are located in the ith and jth spots, by varying i, j and k as previously we can show

$$b_{ij} + b_{ji} = b_{[i+k][j+k]} + b_{[j+k][i+k]} \tag{12}$$

for all i, j and k, where $[i+k] = (i+k) \mod r$. Hence we make the following definitions,

$$\begin{aligned}
a &\triangleq a_1 = a_2 = \cdots = a_r \\
b &\triangleq b_{11} = b_{22} = \cdots = b_{rr} \\
c_1 &\triangleq b_{12} + b_{21} = b_{23} + b_{32} = \cdots = b_{[r-1]r} + b_{r[r-1]} = b_{r1} + b_{1r} \\
c_2 &\triangleq b_{13} + b_{31} = b_{24} + b_{42} = \cdots = b_{[r-1]1} + b_{1[r-1]} = b_{r2} + b_{2r} \\
&\vdots \qquad\qquad \vdots \\
c_k &\triangleq b_{1[1+k]} + b_{[1+k]1} = \cdots = b_{rk} + b_{1k}
\end{aligned}$$

where k is defined in the remainder as

$$k \triangleq \begin{cases} \frac{r}{2} & r\,\text{even} \\ \frac{r-1}{2} & r\,\text{odd.} \end{cases}$$

Using the definitions above, we can rewrite (8) as

$$\begin{aligned}
s(z) &= a(z_1 + z_2 + \cdots + z_r) \\
&+ b(z_1^2 + z_2^2 + \cdots + z_r^2) \\
&+ c_1(z_1 z_2 + z_2 z_3 + \cdots + z_r z_1) \\
&+ c_2(z_1 z_3 + z_2 z_4 + \cdots + z_r z_2) \\
&\vdots \qquad\qquad \vdots \\
&+ c_k(z_1 z_{1+k} + z_2 z_{2+k} + \cdots + z_r z_k) + O(\|z\|^3).
\end{aligned} \tag{13}$$

It is obvious by inspection that $s(z)$ is invariant under rotation as advertised. Observe that the first order term vanishes if we assume zero average mistuning, $\sum_{i=1}^{r} z_i = 0$. Equation (13) can be rewritten more compactly as

$$s(z) = a \sum_{i=1}^{r} z_i + z' \mathcal{S} z + O(\|z\|^3) \tag{14}$$

where $\mathcal{S}$ is defined for even and odd r, respectively,

$$\mathcal{S} = \begin{bmatrix} b & \frac{c_1}{2} & \frac{c_2}{2} & \dots & c_k & \dots & \frac{c_2}{2} & \frac{c_1}{2} \\ \frac{c_1}{2} & b & \frac{c_1}{2} & \frac{c_2}{2} & \dots & c_k & \dots & \frac{c_2}{2} \\ \frac{c_2}{2} & \frac{c_1}{2} & b & \frac{c_1}{2} & \frac{c_2}{2} & \dots & c_k & \dots \\ & & \ddots & & \ddots & & & \\ & & & & \ddots & & \ddots & \\ \frac{c_1}{2} & \frac{c_2}{2} & \dots & c_k & \dots & \frac{c_2}{2} & \frac{c_1}{2} & b \end{bmatrix} \quad or \quad \begin{bmatrix} b & \frac{c_1}{2} & \frac{c_2}{2} & \dots & \frac{c_k}{2} & \frac{c_k}{2} & \dots & \frac{c_2}{2} & \frac{c_1}{2} \\ \frac{c_1}{2} & b & \frac{c_1}{2} & \frac{c_2}{2} & \dots & \frac{c_k}{2} & \frac{c_k}{2} & \dots & \frac{c_2}{2} \\ \frac{c_2}{2} & \frac{c_1}{2} & b & \frac{c_1}{2} & \frac{c_2}{2} & \dots & \frac{c_k}{2} & \frac{c_k}{2} & \dots \\ & & \ddots & & \ddots & & & & \\ & & & & \ddots & & \ddots & & \\ \frac{c_1}{2} & \frac{c_2}{2} & \dots & \frac{c_k}{2} & \frac{c_k}{2} & \dots & \frac{c_2}{2} & \frac{c_1}{2} & b \end{bmatrix}$$

and z' denotes the transpose of z. Notice that $\mathcal{S}$ is real, symmetric and cyclic, a very special structure caused by the symmetry of the problem.

We now take a step back to consider our results thus far. By using symmetry arguments, we have reduced *'find new stability boundaries'* to *'find r/2 + 2 stability coefficients'*. Once we have found $a, b, c_1, c_2, \dots, c_k$, the analysis problem is solved up to second order in z. This is a very useful simplification. Furthermore, we can make very interesting and useful conclusions based on equation (14). Some of these conclusions are listed below:

i. The structure proved above is *independent* of model type, hence it is true for *any* model including dynamical system, imposed sinusoidal motion or CFD models. The only requirement is a $2\pi/r$ rotation symmetry group.

ii. When restricted to zero average, mistuning appears as a second order effect.

iii. To prove equation (14) we assumed a rotational symmetry. However, the second order term, $z'\mathcal{S}z$ also has a sign and reflection symmetry. In other words, $z'\mathcal{S}z$ is invariant under $z \mapsto -z$ and $(z_1, z_2, \dots, z_r) \mapsto (z_r, z_{r-1}, \dots, z_2, z_1)$. This implies that (for a zero average mistuning) sign and reflection appear as third order effects. So there is a hierarchy of stability effects; tuned (average) terms appear in the first order, zero average mistuning is a second order phenomena and mistuning reflection is of third order.

It remains to determine the stability coefficients $a, b, c_1, \dots, c_k$, we present two methods to do so in the following subsections.

4.1 Method A: Computing Eigenvalue Derivatives

Determining $a, b, c_1, \dots, c_k$ can be easily viewed as a derivatives of eigenvalues with respect to parameters problem. The approach below has some nice properties, it only requires information at $z = 0$ (the tuned case) and is easily adjusted for different types of mistuning with a minimum of computation.

Method A is based on *any* discrete blade model (1) where the resulting Jacobian

$$M(U, z) \triangleq \frac{\partial f}{\partial x}(x_0(U, z), U, z), \tag{15}$$

has the property that the quantities

$$\begin{array}{ccc} M(U_{crit}(0),0), & \dfrac{\partial M}{\partial z_i}(U_{crit}(0),0), & \dfrac{\partial^2 M}{\partial z_i \partial z_j}(U_{crit}(0),0), \\ \dfrac{\partial M}{\partial U}(U_{crit}(0),0), & \dfrac{\partial^2 M}{\partial U^2}(U_{crit}(0),0), & \dfrac{\partial^2 M}{\partial U \partial z_i}(U_{crit}(0),0) \end{array} \tag{16}$$

can be computed (analytically or numerically) for all i and j. Practically, the requirement above is not easily satisfied for complex models (1). Specifically, $M(U,z)$ cannot be computed for most CFD models.

To define $s(z)$ in terms of eigenvalue derivatives, consider the Taylor expansion of $h(U,z)$ (Figure 3) about $U_{crit}(0)$ for any z in Ω,

$$\begin{aligned} h(U,z) &= h(U_{crit}(0),z) + \left[\frac{\partial h}{\partial U}(U_{crit}(0),z)\right](U - U_{crit}(0)) \\ &+ \frac{1}{2}\left[\frac{\partial^2 h}{\partial U^2}(U_{crit}(0),z)\right](U - U_{crit}(0))^2 + O(|U - U_{crit}(0)|^3). \end{aligned} \tag{17}$$

Figure 3 illustrates a case where eigenvalues cross between $U_{crit}(0)$ and $U_{crit}(z)$. However, in Assumption 1 we assume that $s(z)$ is smooth for all z in Ω which implies that eigenvalues cannot cross and (17) holds in Ω. Denote partials with respect to U by subscripts,

$$h(z) \triangleq h(U_{crit}(0),z) \tag{18}$$

$$h_u(z) \triangleq \frac{\partial h}{\partial U}(U_{crit}(0),z) \tag{19}$$

$$h_{uu}(z) \triangleq \frac{\partial^2 h}{\partial U^2}(U_{crit}(0),z) \tag{20}$$

By definitions of U_{crit} and s (see equations (4) and (5)), using (18), (19), (20) and substituting $U = U_{crit}(z)$ into equation (17) we obtain

$$0 = h(U_{crit}(z),z) = h(z) + h_u(z)s(z) + \frac{1}{2}h_{uu}(z)s^2(z) + O(\|z\|^3) \tag{21}$$

where the error estimate is derived by noting that $s(z) = O(\|z\|)$.

We can apply identical symmetry arguments to $h(z), h_u(z), h_{uu}(z)$ as we applied to $s(z)$, thus

$$h(z) = h(0) + \bar{h}\sum_{i=1}^{r} z_i + z'Hz + O(\|z\|^3) \tag{22}$$

$$h_u(z) = h_u(0) + \bar{h}_u\sum_{i=1}^{r} z_i + z'H_u z + O(\|z\|^3) \tag{23}$$

$$h_{uu}(z) = h_{uu}(0) + \bar{h}_{uu}\sum_{i=1}^{r} z_i + z'H_{uu} z + O(\|z\|^3) \tag{24}$$

where $h(0) = 0$, $h_u(0), h_{uu}(0), \bar{h}, \bar{h}_u, \bar{h}_{uu}$ are constant and the constant matrices H, H_u, H_{uu} have the same structure as $\mathcal{S}$—real, symmetric and cyclic.

Substituting (14), (22),(23) and (24) into (21) yields

$$\left[\bar{h} + ah_u(0)\right]\sum_{i=1}^{r} z_i + z'\left[H + h_u(0)\mathcal{S} + (a\bar{h}_u + a^2 h_{uu}(0)/2)E\right]z + O(\|z\|^3) = 0, \tag{25}$$

where E is a full matrix of unit entries which is generated by quadratic cross terms: $(\sum_{i=1}^{r} z_i)^2 = z'Ez$. Equation (25) holds for all z in Ω hence

$$\bar{h} + ah_u(0) = 0 \tag{26}$$

and by Lemma B.1,

$$H + h_u(0)\mathcal{S} + (a\bar{h}_u + a^2 h_{uu}(0)/2)E = 0. \tag{27}$$

It follows from Assumption 1 that $h(U,0)$ intersects the origin at $U_{crit}(0)$ in a non-degenerate fashion (*not* as shown in Figure 4), so $h_u(0) = \partial h(U_{crit}(0),0)/\partial u$ is non-zero. Therefore,

$$a = -\frac{\bar{h}}{h_u(0)}, \quad \mathcal{S} = \frac{1}{h_u(0)}\left(-H + \frac{\bar{h}}{h_u(0)}\left[\bar{h}_u - \frac{\bar{h}\,h_{uu}(0)}{2h_u(0)}\right]E\right). \tag{28}$$

By definition, $h(U,z) = \mathrm{Re}[\lambda_p(U,z)]$ where λ_p is the least stable (maximal real part) eigenvalue of $M(U_{crit}(0),0)$. By Assumption 1 it remains the least stable eigenvalue for z in Θ the neighbourhood of interest—no eigenvalue switching as in Figure 5. Using definitions (18), (19), (20) and differentiating equations (22), (23) and (24) with respect to z and U yield equations which hold for any j (by symmetry)

$$\begin{aligned}
\bar{h} &= \mathrm{Re}\left[\frac{\partial \lambda_p}{\partial z_j}(U_{crit}(0),0)\right], & (29)\\
\zeta &= \mathrm{Re}\left[\frac{\partial^2 \lambda_p}{\partial z_j^2}(U_{crit}(0),0)\right], & (30)\\
\varrho_i &= \mathrm{Re}\left[\frac{\partial^2 \lambda_p}{\partial z_j \partial z_{j+i}}(U_{crit}(0),0)\right], & (31)\\
h_u(0) &= \mathrm{Re}\left[\frac{\partial \lambda_p}{\partial U}(U_{crit}(0),0)\right], & (32)\\
\bar{h}_u &= \mathrm{Re}\left[\frac{\partial^2 \lambda_p}{\partial U \partial z_j}(U_{crit}(0),0)\right], & (33)\\
h_{uu}(0) &= \mathrm{Re}\left[\frac{\partial^2 \lambda_p}{\partial U^2}(U_{crit}(0),0)\right], & (34)
\end{aligned}$$

where ζ and ϱ_i are the entries of H and appear in the same format as b and c_i, the entries of $\mathcal{S}$ in equation (14). In the above we can set j to unity for convenience. Substituting equations (29) through (34) into (28) yields expressions for the coefficients $a, b, c_1, \ldots, c_k$ in terms of eigenvalue derivatives,

$$\begin{aligned}
a &= -\frac{\{\partial\lambda_p/\partial z_1\}}{\{\partial\lambda_p/\partial U\}}, & (35)\\
b &= \frac{1}{\{\partial\lambda_p/\partial U\}}\left(-\left\{\frac{\partial^2\lambda_p}{\partial z_1^2}\right\} + \frac{\{\partial\lambda_p/\partial z_1\}}{\{\partial\lambda_p/\partial U\}}\left[\left\{\frac{\partial^2\lambda_p}{\partial U \partial z_1}\right\} - \frac{\{\partial\lambda_p/\partial z_1\}\{\partial^2\lambda_p/\partial U^2\}}{2\{\partial\lambda_p/\partial U\}}\right]\right), & (36)\\
c_i &= \frac{1}{\{\partial\lambda_p/\partial U\}}\left(-\left\{\frac{\partial^2\lambda_p}{\partial z_1 \partial z_{1+i}}\right\} + \frac{\{\partial\lambda_p/\partial z_1\}}{\{\partial\lambda_p/\partial U\}}\left[\left\{\frac{\partial^2\lambda_p}{\partial U \partial z_1}\right\} - \frac{\{\partial\lambda_p/\partial z_1\}\{\partial^2\lambda_p/\partial U^2\}}{2\{\partial\lambda_p/\partial U\}}\right]\right) & (37)
\end{aligned}$$

where all derivatives above are evaluated at $(U,z) = (U_{crit}(0),0)$ and $\{x\}$ denotes the real part of x. It only remains to actually compute the right hand sides of equations (35), (36) and (37).

These computations are performed using the classic results of Lancaster [12] for the derivatives of eigenvalues with respect to matrix parameters. Specifically, the symmetric derivatives can be written as

$$\frac{\partial \lambda_p}{\partial \mu}(U_{crit}(0),0) = \rho_{pp}, \tag{38}$$

$$\frac{\partial^2 \lambda_p}{\partial \mu^2}(U_{crit}(0),0) = U_p' \left[\frac{\partial^2 M}{\partial \mu^2}(U_{crit}(0),0)\right] V_p + 2\sum_{k\in I} \frac{\rho_{pk}\rho_{kp}}{\lambda_p - \lambda_k} \tag{39}$$

where

$$\rho_{ij} = U_i'[\partial M(U_{crit}(0),0)/\partial \mu]V_j,$$

U_i, V_i are the ith left and right eigenvectors of $M(U_{crit}(0),0)$, the summation is taken over

$$I = \{k : \lambda_k(U_{crit}(0),0) \neq \lambda_p(U_{crit}(0),0), k \in (1,2,\ldots,rm)\}$$

and μ can take on the values $z_1, z_2, \ldots, z_r$ or U. Using the chain rule we can derive a formula for asymmetric derivatives,

$$\frac{\partial^2 \lambda_p}{\partial \mu \partial \nu}(U_{crit}(0),0) = \frac{1}{2}\left(\frac{\partial^2 \lambda_p}{\partial \eta^2}(U_{crit}(0),0) - \frac{\partial^2 \lambda_p}{\partial \mu^2}(U_{crit}(0),0) - \frac{\partial^2 \lambda_p}{\partial \nu^2}(U_{crit}(0),0)\right) \tag{40}$$

where μ and ν can take on values $z_1, z_2, \ldots, z_r$ or U and η is a variation in both μ and ν (set both ν and μ equal to η). This reduces the asymmetric partials to three symmetric partials which can be computed as in equation (39). For example, $\partial^2\lambda_p/\partial z_1 \partial z_2$ is derived by setting μ to z_1, ν to z_2 and equating z_1 and z_2 to η, then

$$\frac{\partial^2 \lambda_p}{\partial \eta^2} = \frac{\partial^2 \lambda_p}{\partial z_1^2} + \frac{\partial^2 \lambda_p}{\partial z_2^2} + 2\frac{\partial^2 \lambda_p}{\partial z_1 \partial z_2}. \tag{41}$$

Equations (38), (39) and (40) hold when the eigenvalue $\lambda_p(U_{crit}(0),0)$ is simple, meaning that its Jordan block has simple (diagonal) form. In particular, if $\lambda_p(U_{crit}(0),0)$ is distinct then these equations are valid. We do not consider the non-distinct case since Assumption 1 is violated when $\lambda_p(U_{crit}(0),0)$ is non-distinct.

At this point it is useful to make some comments about when we expect to encounter non-distinct eigenvalues. The symmetry of the problem implies that the Jacobian matrix $M(U_{crit}(0),0)$ has a block circular structure (see Appendix A). Generically, such matrices have distinct eigenvalues and so generic models will have distinct eigenvalues. However, not all models are generic. For example, the quasi-steady model in Appendix A is degenerate because it only includes coupling between adjacent blades and the resulting block circulant Jacobian (equation (67)) has only three non-zero blocks. In this case some of the eigenvalues are non-distinct. This leads to two cases: if the least stable eigenvalue is distinct then the fact that other eigenvalues may be non-distinct is irrelevant. If it is not distinct, then the least stable eigenvalue/s will typically be simple and will travel smoothly with parameters. As a result Lancaster's equations ((38), (39) and (40)) still apply and so we need only keep track of multiple eigenvalues to extend the analysis. (In the quasi-steady model, only a few of the eigenvalues repeat and so the least stable eigenvalue is usually distinct. For parameters in this paper, non-distinct least stable eigenvalues were only observed for $r = 6$ or $r = 22$.) Notice that the above is actually the exact opposite of what one would expect for unconstrained matrices. If we do not restrict attention to circulant matrices then the class of matrices with non-distinct eigenvalues is generically non-simple. For a detailed discussion of these issues see Appendix B.

To apply (38), (39) and (40) we need to compute λ_i, U_i and V_i, the eigenvalues and left, right eigenvectors of $M(U_{crit}(0), 0)$ for all i. Since $M(U_{crit}(0), 0)$ has a block circular structure (Appendix A) we can apply the methods of Appendix B to compute the eigenvalues and vectors. These methods provide a significant reduction in computational complexity: instead of solving the $rm \times rm$ eigenvalue/vector problem (m is the number of states per blade) where computation time increases as $(rm)^3$, we solve an $m \times m$ eigenvalue/vector problem r times with resulting computation time rm^3, a savings of r^2. These methods also avoid the numerical difficulties inherent in solving eigenvalue/vector problems for matrices with non-distinct eigenvalues.

We conclude this subsection by summarizing the above procedure for the quasi-steady model introduced in Appendix A.

- Step 1: Derive the matrix $M(U, z)$ — Appendix A, equation (67).
- Step 2: Compute the eigenvalues of $M(U, 0)$ for $U \in [U_0, U_1]$, the range of interest, by the methods of Appendix B.
- Step 3: From step 2, construct $h(U, 0)$ the maximal real part of eigenvalues at every $U \in [U_0, U_1]$.
- Step 4: Find $U_{crit}(0)$, the point where $h(U, 0)$ changes sign. Suggested methods to do so are a bisection algorithm or the Newton-Raphson method.
- Step 5: Compute left and right eigenvectors (U_i, V_i) of $M(U_{crit}(0), 0)$ using Appendix B.
- Step 6: Evaluate equations (38),(39) and (40) as μ and ν vary over $z_1, z_2, \ldots, z_r$ and U.
- Step 7: Substitute the results of step 6 into (35), (36) and (37) to compute the stability coefficients $a, b, c_1, \ldots, c_k$.

Notice that all steps above only require information at the tuned point $z = 0$. Mathematica code that implements method A is available by request from the author.

4.2 Method B: Finite Difference

For some models (1) it is not possible to compute the quantities (16). In particular, it is impractical to compute $M(U, z)$ and its derivatives for computational fluid dynamics (CFD) models due to their complexity and large number of states.

Given any model (1) which can accurately predict $s(z)$ for any given mistuning z, estimate the coefficients $a, b, c_1, \ldots, c_k$ by finite difference. From equation (13)

$$a = \frac{\partial s}{\partial z_1}(0) \approx \frac{s(\epsilon, 0, \ldots, 0)}{\epsilon} \tag{42}$$

$$b = \frac{1}{2}\frac{\partial^2 s}{\partial z_1^2}(0) \approx \frac{s(2\epsilon, 0, \ldots, 0) - 2s(\epsilon, 0, \ldots, 0)}{2\epsilon^2} \tag{43}$$

$$c_i = \frac{\partial^2 s}{\partial z_1 \partial z_{1+i}}(0) \approx \frac{s(\epsilon, 0, \ldots, 0, \epsilon, 0, \ldots, 0) - 2s(\epsilon, 0, \ldots, 0)}{\epsilon^2} \tag{44}$$

where in the last equation the second ϵ in $s(\epsilon, 0, \ldots, 0, \epsilon, 0, \ldots, 0)$ appears in the $(i+1)$th spot and ϵ is small. To obtain $a, b, c_1, \ldots, c_k$ we need to run model (1) a total of $r/2 + 2$ times so as to form the right hand side of equations (42), (43) and (44). Once these runs have been completed, the analysis question is solved and the effect of all other types of mistuning is known up to second order in z. To estimate the required coefficients we need a model that predicts $s(z)$ accurately so that meaningful second order finite differences may be formed. Consequently, the method above is susceptible to numerical noise which may cause large errors when attempting to numerically determine second order derivatives.

5 Synthesis

Once the analysis question has been solved, the next obvious task is Synthesis: when is mistuning beneficial? If it is beneficial what is the optimal mistuning? In order to address these questions define the notion of optimal mistuning.

First it is necessary to decide which "type" of mistuning will be used. Various possibilities include blade stiffness, blade angle of attack, stator shape, cowling clearance and many other forms of mistuning. In this section it is assumed that the type of mistuning has been pre-determined and we will not concern ourselves with optimizing over type. From a practical standpoint we wish to maximize the stability extension $s(z)$ while keeping the "side effects" of mistuning acceptable. Here side effects refers to everything from increased weight and manufacturing cost to a decrease in operating range [17] due to mistuning. So, to solve the true optimal problem we would quantify all the possible side effects (such as cost, weight, operating range and many others) and form a constrained optimization problem where we maximize $s(z)$ subject to the constraint that side effects remain below some practically motivated boundary. Clearly, such an approach is too ambitious. At present we do not know how to quantify increase in cost, operating range and other factors as a function of mistuning. Furthermore, there is no way to compose a complete list of all possible side effects. Consequently, an optimization problem thus obtained will almost certainly be untractable due to complexity of constraints motivated by acceptable side effects. To avoid these difficulties, we simply restrict the size of mistuning and assume that resulting side effects are acceptable if z is sufficiently small. In future research we will begin to include physically motivated constraints to account for important side effects.

It remains to define the size of mistuning. To motivate the norm chosen consider a blade stiffness mistuning. Manufacturing and weight considerations would allow some small variation in each blade, so: $|z_i| \leq \epsilon$ for all i. This leads to a natural optimization problem constrained by the infinity norm on z:

3 *Optimization: Maximize* $s(z) = a\sum_{i=1}^{r} z_i + z'Sz + O(\|z\|^3)$ *subject to* $\|z\|_\infty \leq \epsilon$.

Having formulated the optimization problem we can determine if mistuning is beneficial. Of course it is understood that we are judging the benefit based on the model chosen to represent the jet engine.

We show that mistuning only makes sense if ϵ is sufficiently large compared to a ratio of linear (a) to quadratic ($b, c_1, \ldots, c_k$) terms in equation (13). Recall equation (14),

$$s(z) = a\sum_{i=1}^{r} z_i + z'Sz + O(\|z\|^3) \tag{45}$$

where S is a real, symmetric, cyclic matrix containing the quadratic coefficients $b, c_1, \ldots, c_k$ and z' is the transpose of z. Let

$$\begin{array}{llccl} \bar{z} & \textit{solution to:} & \max & a\sum_{i=1}^{r} z_i & \text{subject to} \quad \|z\|_\infty \leq 1, \\ z^* & \textit{solution to:} & \max & z'Sz & \text{subject to} \quad \|z\|_\infty \leq 1,\ \sum_{i=1}^{r} z_i = 0. \end{array}$$

By inspection, $\bar{z} = (1, 1, \ldots, 1)$, and corresponds to a mean *tuned* increase in parameters (assume $a > 0$, else reverse sign of $\bar{z}$). Conversely, z^* corresponds to a zero average mistuning which optimizes $s(z)$ up to second order (assume $S \not\leq 0$ and hence $z^* \neq 0$). If we impose a zero average restriction and truncate third order terms, then optimization $\{3\}$ has solution ϵz^*. Furthermore, $\|z^*\|_\infty = 1$ else $z^{*\prime}Sz^*$ may be increased by $z^* \mapsto (1+\delta)z^*$.

Now ask the following practically motivated question: given an allowable size of mistuning ϵ is it better to apply the optimal zero average mistuning z^* or just increase parameters all around by a tuned amount $\bar{z}$? So compare

$$s(\alpha\bar{z}) = (ar)\alpha + \left(\bar{z}'S\bar{z}\right)\alpha^2 + O(\alpha^3) \tag{46}$$

$$s(\alpha z^*) = 0 + \left(z^{*\prime}Sz^*\right)\alpha^2 + O(\alpha^3) \tag{47}$$

where $\alpha > 0$ is the size of mistuning. For sufficiently small α the tuned stability extension $s(\alpha\bar{z})$ is always greater since it has a non-zero linear term $(ar)\alpha$. However, $z^{*\prime}Sz^*$ is typically greater than $\bar{z}'S\bar{z}$ because z^* is the constrained quadratic optimum (note $z^* \neq \bar{z}$) and hence $(z^{*\prime}Sz^*)\alpha^2$ eventually overtakes $(ar)\alpha + (\bar{z}'S\bar{z})\alpha^2$ (see Figure 6). Such a crossover occurs at

$$\alpha^* = \frac{ra}{z^{*\prime}Sz^* - \bar{z}'S\bar{z}}. \tag{48}$$

Based on this second order analysis: if $\alpha^* < \epsilon$ then ϵ sized zero average mistuning is worthwhile ($s(\epsilon z^*) > s(\epsilon\bar{z})$), otherwise it is not. Rephrasing, a zero average mistuning is only worthwhile if it is bigger then α^*. Of course the second order approximation may fail at α^* if α^* is too large in which case we can not make any claims. Notice that α^* is small if second order coefficients $(b, c_1, \ldots, c_k)$ dominate the first order coefficient a.

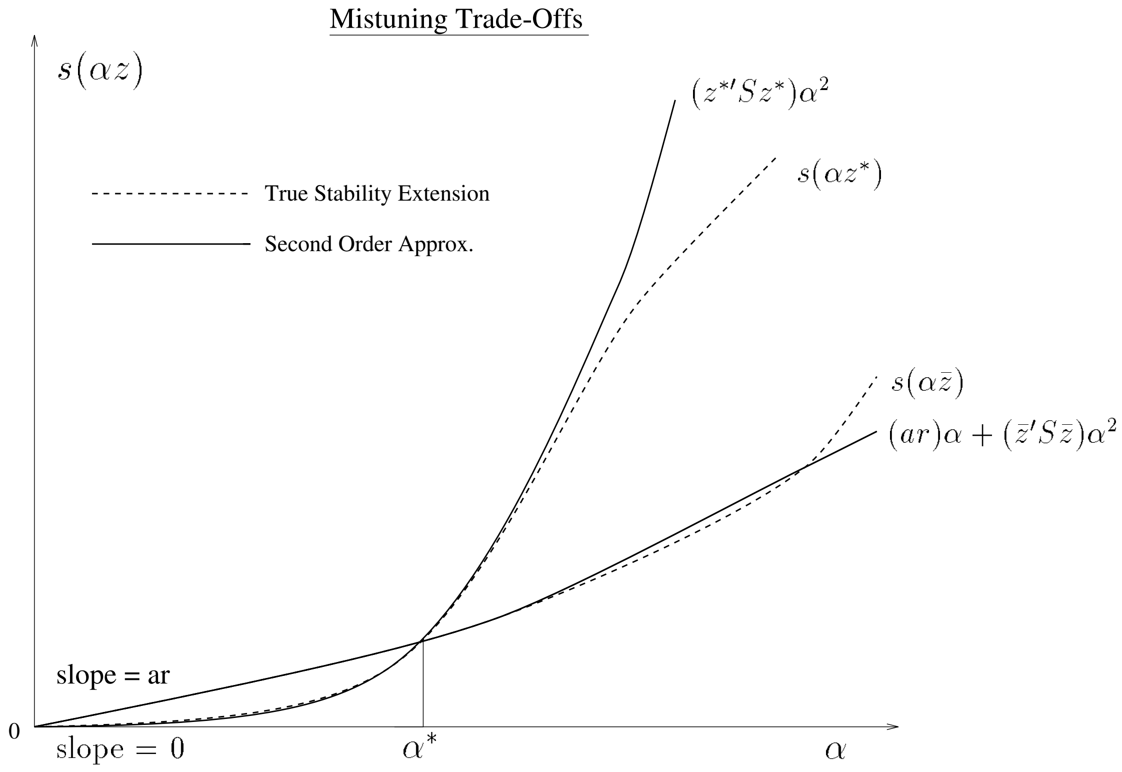

Figure 6: Worthwhile mistuning lower bound

It is now clear that results in this paper allow the reader to judge *when* to apply mistuning, based on the model (1). However, they also determine *which* mistuning should be applied. This is done by solving the optimization {3} up to second order—a standard linear constraint quadratic programming problem. There exist numerical techniques [1] which can find global maximums of

$a\sum_{i=1}^r z_i + z'Sz$ subject to $\|z\|_\infty \le \epsilon$. Current software (supplied by F. Al-Khayyal, T. Van Voorhis and the company CPLEX) can usually solve problems up to $r \approx 30$. Larger optimizations take too long ($r = 60$ is projected to take approximately 30 years) but it is possible that computation time can be decreased dramatically by utilizing the special structure of S. In fact, because general quadratic programs are provably NP hard [13], solutions to large optimal mistuning problems will not be possible *unless* one exploits the special symmetry and structure of the mistuning problem. Such exploitation of problem structure—and the resulting dramatic decrease in computational complexity—is demonstrated in the next section.

6 A Combinatorial Optimization with Structure

Mistuning can, at first glance, lead to notoriously difficult optimization problems. For example, suppose n blades are made and these blades have a set of mistuning values (say stiffness variations) $y_1, y_2, \ldots, y_n$ due to machining tolerances. Given the stability coefficients $a, b, c_1, c_2, \ldots, c_k$ and assuming y_i's are known (measurable) what is arrangement of the r blades that maximizes stability? If we wanted to solve the problem exhaustively, we would have to check n permute r or $n!/(n-r)!$ possibilities. Clearly this is not practical for large r or n; even the special case $n = r$ requires $r!$ operations. A possible solution lies in the problem structure—exploiting such structure can result in tremendous complexity reduction. Specifically, circular structure of the mistuning problem *and* the additional structure of the stability coefficients c_i found in the quasi-steady model (see Section 7, Table 1) allows solution of the $n = r$ combinatorial optimization in closed form.

Consider the set of models where stability coefficients satisfy the relation

$$c_1 > c_2 > \cdots > c_{k-1} > c_k, \quad r \quad \text{odd}, \tag{49}$$
$$c_1 > c_2 > \cdots > c_{k-1} > 2c_k, \quad r \quad \text{even}. \tag{50}$$

Condition (49) or (50) holds for the quasi-steady model (Appendix A) over a fairly broad range of parameter values. There is no reason for this condition to hold for other models, yet there is also no reason to suppose that such structure is specific to the quasi-steady model. When condition (49) or (50) holds, the problem

4 <u>*Combinatorial Optimization:*</u> *Given mistuning values $(y_1, y_2, \ldots, y_r)$, the stability coefficients $(a, b, c_1, \ldots, c_k)$ that satisfy condition (49) or (50) and the resulting matrix $\mathcal{S}$ of equation (14); maximize $s(z) = a\sum_{i=1}^r z_i + z'\mathcal{S}z$ subject to $z \in \Pi = \{z : z = (y_{l_1}, y_{l_2}, \ldots, y_{l_r}), l_i \ne l_j, \forall i \ne j\}$.*

may be solved closed form. Optimization $\{4\}$ is not restricted to mistuning applications, an identical optimization arises in computer science—related to optimal arrangement of records to be searched—and its statement and terse solution can be found in Knuth [11, p.405, Q18 & Q20]. Optimal solutions are all rotations and reflections of the "pyramid" arrangement $z = (z_1, z_2, \ldots, z_r)$ where $z_{k+1} \ge z_k \ge z_{k+2} \ge z_{k-1} \ge \cdots \ge z_{r-1} \ge z_2 \ge z_r \ge z_1$ for r even or $z_{k+1} \ge z_k \ge z_{k+2} \ge z_{k-1} \ge \cdots \ge z_2 \ge z_{r-1} \ge z_1 \ge z_r$ for r odd (see Figure 7). So computational complexity drops from $r!$ to $r \log r$ which is the sorting time for r objects [11].

The proof presented here follows Knuth [11]. We show the r odd case but r even is almost identical, the only difference being the factor of two that multiplies c_k in (50). First note that the solution to $\{4\}$ is independent of the coefficients a and b because the relevant terms $a\sum_{i=1}^r z_i$ and $b\sum_{i=1}^r z_i^2$ are invariant under permutations of z. So without loss of generality we may consider the objective function $z'\mathcal{C}z = z'(\mathcal{S} - bI)z$ which depends on coefficients c_i only. Now, for any z make

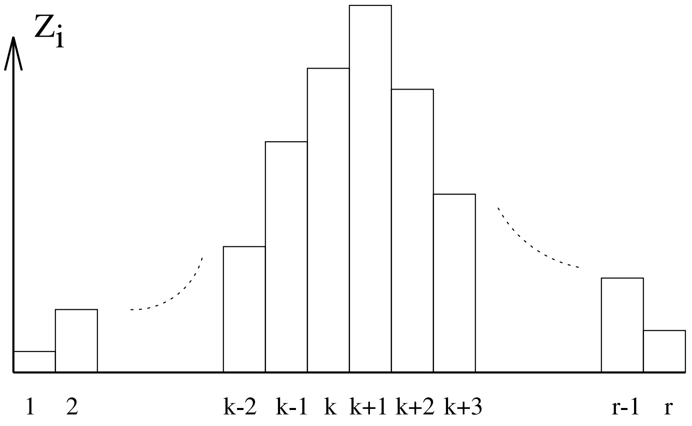

Figure 7: Optimal "pyramid" arrangement (r even).

one of two identifications (here β and δ are placeholder variables)

$$z = (\alpha_1, \alpha_2, \ldots, \alpha_k, \beta, \gamma_k, \ldots, \gamma_2, \gamma_1) \tag{51}$$
$$z = (\alpha_1, \alpha_2, \ldots, \alpha_k, \gamma_k, \ldots, \gamma_2, \gamma_1, \delta) \tag{52}$$

and define the sets

$$A = \{i : \alpha_i < \gamma_i, i \in (1, 2, \ldots, k)\}, \tag{53}$$
$$B = \{i : \alpha_i = \gamma_i, i \in (1, 2, \ldots, k)\}, \tag{54}$$
$$C = \{i : \alpha_i > \gamma_i, i \in (1, 2, \ldots, k)\}. \tag{55}$$

Consider switching α_i and γ_i when $\alpha_i > \gamma_i$, hence switch for all $i \in C$. For both (51) and (52) it can be shown that the resulting change in the objective function $z'\mathcal{C}z$ is given by

$$\Delta = \sum_{i \in C, j \in A} \left(c_{|i-j|} - c_{l(i,j)}\right)(\gamma_j - \alpha_j)(\alpha_i - \gamma_i) \tag{56}$$

where

$$l(i,j) = \begin{cases} i + j - h & , \quad i + j - h \leq k \\ r - (i + j - h) & , \quad i + j - h > k. \end{cases} \tag{57}$$

and h is 1 or 0 depending on whether we consider (51) or (52), respectively. It follows that $|i - j| < l(i,j)$ for all i, j in $(1, 2, \ldots, k)$. Hence $c_{|i-j|} > c_{l(i,j)}$ by condition (49), and the terms $(\gamma_j - \alpha_j)$ and $(\alpha_i - \gamma_i)$ are strictly positive by definition of sets A and C. Consequently, $\Delta > 0$ unless either A or C is empty. In other words, we can improve on z in (51) or (52) if both A and C are non-empty. It turns out that only the "pyramid" arrangement of Figure 7 has either A or C empty for all rotations and reflections, hence it is the only arrangement that cannot be improved by the construction (49–57).

Next, recall that optimums come in sets of $2r$—if z^* is an optimum then so is any rotation or reflection of z^*. (Since a reflection about z_i^* is equivalent to a reflection about z_1^* and $2(i-1)$ rotations, we really only have one reflection and r rotations for a total of $2r$ equivalent optimums.) So suppose an optimal solution z^* of problem $\{4\}$ is not a rotation or reflection of the pyramid arrangement. Rotate z^* so that $z_p^* = \max_i z_i^*$ appears in the $(k+1)$th spot (if there is more then one maximum then pick any of these maxima) and reflect z^* about z^*_{k+1} if $z^*_k < z^*_{k+2}$. These two operations yield an equivalent optimum and imply $z^*_{k+1} \geq z^*_k \geq z^*_{k+2}$.

Since z^* is not a rotation or reflection of the "pyramid" arrangement then one of the inequalities in the top row of (58) must fail. The middle and bottom row correspond to the same chain of inequalities using the relabeling of (51) and (52), respectively,

$$\begin{bmatrix} z^*_{k+1} \\ \beta \\ \gamma_k \end{bmatrix} \geq \begin{bmatrix} z^*_k \\ \alpha_k \\ \alpha_k \end{bmatrix} \geq \begin{bmatrix} z^*_{k+2} \\ \gamma_k \\ \gamma_{k-1} \end{bmatrix} \geq \begin{bmatrix} z^*_{k-1} \\ \alpha_{k-1} \\ \alpha_{k-1} \end{bmatrix} \geq \cdots \geq \begin{bmatrix} z^*_2 \\ \alpha_2 \\ \alpha_2 \end{bmatrix} \geq \begin{bmatrix} z^*_{r-1} \\ \gamma_2 \\ \gamma_1 \end{bmatrix} \geq \begin{bmatrix} z^*_1 \\ \alpha_1 \\ \alpha_1 \end{bmatrix} \geq \begin{bmatrix} z^*_r \\ \gamma_1 \\ \delta \end{bmatrix}. \tag{58}$$

First consider the case where $z^*_{k+1} \neq z^*_k \neq z_{k+2}$, hence $z^*_{k+1} > z^*_k > z^*_{k+2}$. We have assumed z^* is not a "pyramid" arrangement so at least one of the inequalities in (58) must fail. There are two possibilities: either $\alpha_i \geq \gamma_i$ fails in the middle row of (58) for some i or $\gamma_j \geq \alpha_j$ fails in the bottom row of (58) for some j. In the first possibility, $\gamma_i > \alpha_i$ so A is non-empty, but $z^*_k > z^*_{k+2}$ so $\alpha_k > \gamma_k$ and C must be non-empty. Hence Δ of equation (56) is positive, z^* can be improved by the construction of (49–57) and so z^* is not the optimum—a contradiction! Similarly, in possibility two $\alpha_j > \gamma_j$ so C is non-empty, but $\gamma_k > \alpha_k$ and hence A is non-empty. This also contradicts the assumption that z^* is optimal.

Now consider the cases where $z^*_{k+1} \neq z^*_k \neq z_{k+2}$ does not hold. When $z^*_{k+1} = z^*_k$ but $z^*_k \neq z^*_{k+2} \neq z^*_{k-1}$, then $z^*_k > z^*_{k+2}$ because z^*_k is a maximum of z^* and we may reflect so that $z^*_{k+2} > z^*_{k-1}$. Now we apply the same arguments as above except $\gamma_k > \alpha_k$ gets replaced by $\gamma_{k-1} > \alpha_{k-1}$ to ensure A is non-empty for the bottom inequality chain. The same reflection and right shift applies for the next case where $z^*_{k+1} = z^*_k = z^*_{k+2} \neq z^*_{k-1} \neq z^*_{k+3}$ and so on. Notice that we need at least two values of z^* different from the maximal value $z^*_p = \max_i z^*_i$, otherwise all arrangement are optimal. For example, if the mistuning values are $y_1 = y_2 = \cdots = y_{r-1} \neq y_r$ then all arrangements are equivalent by circular symmetry.

7 Results and Applications to a Simple Quasi-Steady Model

Conceptually, there are two *levels* of results in this paper. Level one encompasses a reduction of practical mistuning issues to tractable mathematical questions. This level includes definitions of stability extensions, symmetry arguments, quadratic optimizations, large eigenvalue matrix problems and their reduction to smaller (more tractable) matrix questions. It is stressed that this level is *model independent* and provides a general framework for analyzing and optimizing mistuning. Of course it is understood that no single method can be general enough to encompass all possible cases. However, the method presented in this paper is quite simple. As a result, for specific applications which might fall outside the scope of level one, it becomes obvious how to extend the analysis in question. For example, if it is found that third order terms are important in $s(z)$, then the extension required involves computing third order coefficients and optimizing over cubic terms. Thus the main contribution of this paper is the consistent, systematic approach to mistuning presented.

Level two lies below level one and deals with specific models. Researchers may pick whichever model (equation (1)) they believe captures relevant aerodynamic effects for their specific application. Once a specific model has been picked, symmetry arguments presented (or an extension thereof) can be applied to solve the analysis and synthesis questions. It is hoped that methods in this paper will serve as a guiding principle in choice of relevant models. For example, suppose experiments show that mistuning in a given application has a large effect on stability. Then from Section 5, equation (48), $\alpha^* = ra/(z^{*\prime} S z^* - \bar{z}' S \bar{z})$ must be small. If the model chosen does not have this property then it follows that this model does not accurately predict mistuning.

For the purposes of this paper, we use a quasi-steady model (Appendix A) to present and validate the symmetry arguments. Since this is the simplest model that will display flutter-like instabilities we urge the reader to treat these results with caution. The model used assumes quasi-steady aerodynamics (hence it does not include unsteady fluid dynamics), there is only one degree of freedom and a single blade coupling mechanism. As a result, this model is incapable of capturing complex nonlinear behaviour or important unsteady aerodynamic effects. Nevertheless, this model is still quite useful since the blade coupling included captures one of the major causes of instabilities in blade cascades.

Within the model, we can mistune three quantities, they are stiffness k_i, mass m_i and blade angle of attack β_i. It was noticed that mass and stiffness mistuning result in almost identical behaviour, both in coefficients computed $a, b, c_1, \ldots, c_k$ and in optimization results. Consequently, we only discuss stiffness and angle of attack mistuning. At the end of Section 4.1 we outlined seven steps to compute the coefficients $a, b, c_1, \ldots, c_k$. To illustrate results (which were found to be typical across parameter space) we pick parameters in the quasi-steady model corresponding to a high speed fan with sixteen blades ($r = 16$). Computing eigenvalues and vectors by the methods of Appendix B we can plot $h(U, 0)$ of Step 3, Section 4.1 and a tuned root locus plot (Figure 8). Hence, $U_{crit}(0) = 950.4m/s$. (Here we see the first drawback of the quasi-steady model, it cannot capture

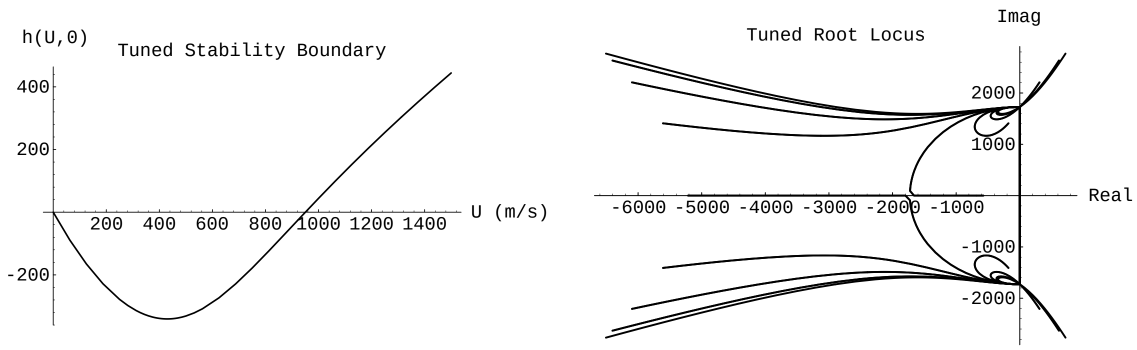

Figure 8: Quasi-steady model: motion of tuned eigenvalues, stability boundary and root locus.

compressible effects and the instability velocity is far too high.) Evaluating steps five through seven (end of Section 4.1) yields the coefficients $a, b, c_1, \ldots, c_k$. Comparison with Method B of Section 4.2 shows that for ϵ sufficiently small in equations (42), (43) and (44), the coefficients computed by Methods A and B fall arbitrarily close to one another (up to machine error) hence results for Method B are not shown.

Mistuning	a	b	c_1	c_2	c_3	c_4	c_5	c_6	c_7	c_8
Stiffness	29.70	55.81	71.99	37.56	8.44	-15.40	-33.93	-47.17	-55.12	-57.77
Angle	-1.83	-1.05	-0.20	-0.10	-0.03	0.03	0.09	0.12	0.14	0.15

Table 1: Analysis coefficients for stiffness and blade angle of attack mistuning

For angle of attack mistuning, it can be shown in closed form (Appendix B) that S (of equation (14)) is negative definite. As a result, for zero average mistuning we have $s(z) \approx z'Sz < 0$ for all $z \neq 0$ (see equation (14)). Hence the quasi-steady model predicts that zero average, angle of attack mistuning can only decrease stability.

In the case of stiffness mistuning, it was found that $\alpha^* = 0.1$ in equation (48). Note that α^* is the crossover where optimal zero average mistuning (accurate to second order) first surpasses a tuned increase, hence it makes no sense to mistune by less then α^*. However, the second order approximation of equation (14) fails at $\alpha \approx 0.08$. Within the second order range, we must conclude that mistuning is not beneficial. Outside the second order range we can not make any claims based on our second order analysis.

We compute stability outside the second order range by brute force. Recall the definitions of the tuned increase and optimal zero average mistuning, $\bar{z}$ and z^*, defined below equation (45). If we compute $s(\alpha\bar{z})$ and $s(\alpha z^*)$ as shown in equations (46) and (47) then we see that $s(\alpha\bar{z})$ continues to increase beyond $\alpha = 0.08$ but $s(\alpha z^*)$ falls sharply as α increases beyond 0.08 (this computation was based on solving for the eigenvalues directly instead of approximating them to second order). Thus, $s(\alpha\bar{z})$ is always greater then $s(\alpha z^*)$ and so the quasi-steady model predicts that second order *optimal* zero average mistuning cannot beat a tuned mean increase. Yet based on experimental results such as [19] we expect mistuning to have a *large* effect on stability, certainly much larger then would be caused by a small tuned increase in stiffness. Our conclusion (modulo obvious considerations such as: mistuning does not have a large effect at *these* parameters) must be that the quasi-steady model is a poor predictor of mistuning which is not surprising considering its simplicity.

To determine the optimal zero average stiffness mistuning, we numerically solve the optimization problem {3} up to second order, subject to the additional constraint $\sum_{i=1}^{r} z_i = 0$. The optimal solution ϵz^* has the form $z^* = (1, 1, \ldots, 1, -1, -1, \ldots, -1)$. In other words, if we have r stiffnesses for r blades, denoted k_1 through k_r, the optimal zero average mistuning is in the first mode: $k_1 = k_2 = \ldots = k_{r/2} = k_0(1+\epsilon)$ and $k_{r/2+1} = \ldots = k_r = k_0(1-\epsilon)$. (Recall that $z'Sz$ has a rotational, reflection and sign symmetry—see last bullet in Section 4—hence any rotation, reflection or sign change of ϵz^* is also optimal). Note that the form of the optimal mistuning is very different from alternate blade mistuning proposed in [14], where $k_1 = k_3 = \ldots = k_{r-1} = k_0(1+\epsilon)$ and $k_2 = k_4 = \ldots = k_r = k_0(1-\epsilon)$. It is predicted that the optimal approach is an order of magnitude better then alternate blade mistuning. Figure 9 shows the appropriate stability boundaries for a 5% mistuning of stiffness. The solid line on the far left represents the tuned stability boundary, it

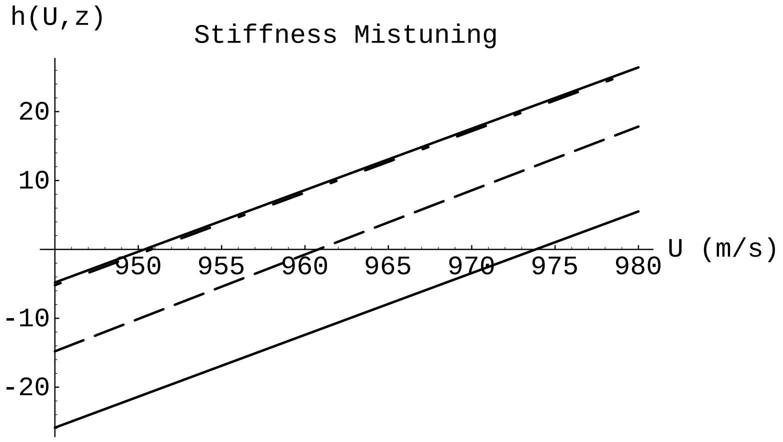

Figure 9: Hierarchy of mistuning boundaries based on quasi-steady model.

intersects the U axis at $U_{crit}(0) = 950.4m/s$. Immediately to the right (dash - dot) is the alternate mistuning boundary, further right we find the optimal zero average stability boundary (dash-dash) and finally on the far right (solid) we have the the tuned increase. There are two things to notice in this figure. First, it makes no sense to introduce mistuning based on the quasi-steady model since the tuned increase is clearly superior to the optimal zero average. Second, there is a huge difference between alternate zero average mistuning and optimal zero average mistuning. Intuitively, alternate mistuning breaks symmetry only mildly. It reduces the single blade spacing $2\pi/r$ symmetry to a two blade spacing $4\pi/r$ symmetry between even and odd blades. By comparison, first mode mistuning destroys *all* circumferential symmetry.

Finally, the optimal mistuning problem seems to have a robust structure. Small changes in system parameters and/or operating conditions such as nominal rotor stiffness, blade mass, and nominal angle of attack do not change the optimal answer. Even though the coefficients $a, b, c_1, \ldots, c_k$ change slightly, their structure remains the same and the optimal solution remains unchanged. Such robustness issues will be addressed rigorously in future research.

8 Conclusion

Results are presented for analyzing and optimizing the stability extensions caused by mistuning. Using mild smoothness conditions and simple symmetry arguments, tough practical issues are reduced to standard, tractable, mathematical problems. Analysis and synthesis problems are solved up to second order in mistuning. Methods are presented to judge when mistuning should be applied. Furthermore, the simplifications presented here allow a researcher to judge easily if his or her model can accurately predict mistuning effects. These techniques are applied to a simple quasi-steady model to illustrate and validate the arguments used. One can conclude that this very simple quasi-steady model does not predict mistuning effects accurately.

Acknowledgements

This work was performed at United Technologies Research Center during the summer of 1996. The author would like to thank M. Myers, D. Gysling, S. Copeland, G. Hendricks and M. Barnett for their willingness to answer questions at inopportune moments. Suggestions and advice from my advisor, R. Murray, are greatfully acknowledged. Thanks are also due to F. Al-Khayyal and T. Van Voorhis at Georgia Tech for their time and numerical optimization code. Numerical solutions would not have been possible without their help.

A Simple Quasi-Steady Model

In this section we introduce the simplest blade cascade model that will go unstable. The primary purpose of this model is to demonstrate the methods in this paper. However, one can draw some interesting, if tentative, conclusions based on this model.

Given a cascade of r blades, assume that each blade (numbered by index i) has one degree of freedom, namely blade bending q_i (see Figure 10). Structural coupling is modeled by a linear spring with stiffness k_i. Incoming velocity U is constant between blades, but β_i is allowed to vary. As a result, we can mistune three quantities: stiffness k_i, mass m_i and blade angle of attack which translates to varying β_i.

Let x_i denote displacement of the ith blade from neutral spring position. Then,

$$m_i\ddot{x}_i + \xi\dot{x}_i + k_i x_i = \mathcal{A}_i \tag{59}$$

where $k_i x_i$ captures the structural force and $\mathcal{A}$ is a combination of quasi-steady aero forces.

Aerodynamic forces are modeled in two parts. Part one deals with quasi-steady aero forces on the ith blade due to its own motion, this force is labeled $\mathcal{F}_i$ and is derived in standard fashion,

$$\mathcal{F}_i = q_\infty c C_{L_\alpha}\gamma_i \tag{60}$$

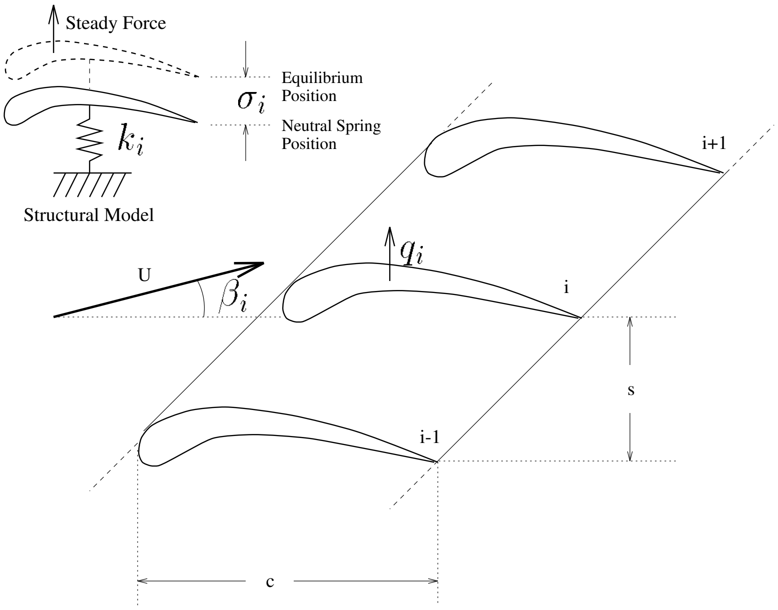

Figure 10: Cascade of blades

where $q_\infty \triangleq \rho U^2/2$, the dynamic pressure, C_{L_α} is the lift curve slope, c is the chord and γ_i is the effective angle of attack due to blade motion. To complete the description of $\mathcal{F}_i$ it remains to compute the angle γ_i. This angle is the flow angle that blade i experiences due to its own motion, or the flow angle in the blade frame of reference. For small $\dot{x}_i$ (60) becomes

$$\mathcal{F}_i = q_\infty c C_{L_\alpha} \left(\beta_i - \frac{\dot{x}_i \cos \beta_i}{U} \right). \tag{61}$$

Part two of the aerodynamic forces deals with forces due to blade coupling. It is assumed that the extra loading on blade i is proportional to the amount of extra flow it must turn, which is in turn proportional to the distance between the $(i-1)$th and $(i+1)$th blade. We label this force as $\mathcal{G}$,

$$\mathcal{G}_i = p q_\infty c \left[\frac{x_{i+1} - x_{i-1}}{2s} \right] \tag{62}$$

where p is the coefficient of loading to extra flow turned and q_∞, c and s play the role of appropriate normalization coefficients. Combining (59), (61), (62) and noting $\mathcal{A} = \mathcal{F} + \mathcal{G}$ yields

$$m_i \ddot{x}_i + \xi \dot{x}_i + k_i x_i = q_\infty c C_{L_\alpha} \left(\beta_i - \frac{\dot{x}_i \cos \beta_i}{U} \right) + p q_\infty c \left[\frac{x_{i+1} - x_{i-1}}{2s} \right]. \tag{63}$$

Let σ_i denote the equilibrium position, as shown in Figure 10. Setting time derivatives to zero in (63) gives

$$k_i \sigma_i = q_\infty c C_{L_\alpha} \beta_i + p q_\infty c \left[\frac{\sigma_{i+1} - \sigma_{i-1}}{2s} \right]. \tag{64}$$

If the cascade is tuned ($k_i = k_0, \beta_i = \beta_0, \forall i$) then (64) collapses to $\sigma_0 = q_\infty c C_{L_\alpha} \beta_0 / k_0$ since all the σ's must equal. However, if the system is not tuned, then the equilibrium changes and

$\sigma_i \neq q_\infty c C_{L\alpha} \beta_0 / k_0$. So, it is stressed once again, that the relevant equilibrium point *does* vary as a function of mistuning. (If the reader is concerned about the existence of an equilibrium solution, note that the vector of σ's satisfies $A\vec{\sigma} = b$ and it can be shown that A is invertible.)

Now let $q_i \triangleq x_i - \sigma_i$, then (63) becomes

$$m_i \ddot{q}_i + \xi \dot{q}_i + k_i q_i = -q_\infty c C_{L\alpha} \frac{\cos\beta_i}{U} \dot{q}_i + p q_\infty c \left[\frac{q_{i+1} - q_{i-1}}{2s} \right]. \tag{65}$$

Equation (65) can be rewritten in desired form as

$$\dot{x} = M(U, z) x \tag{66}$$

where x is redefined as $x = [q_1, \dot{q}_1, q_2, \dot{q}_2, \ldots, q_r, \dot{q}_r]$,

$$M(U, z) = \begin{bmatrix} A_1 & B_1 & 0 & \ldots & 0 & -B_1 \\ -B_2 & A_2 & B_2 & 0 & \ldots & 0 \\ & \ddots & & \ddots & & \\ & & \ddots & & \ddots & \\ B_r & 0 & \ldots & 0 & -B_r & A_r \end{bmatrix}, \tag{67}$$

$$A_i(U, z_i) = \begin{bmatrix} 0 & 1 \\ -\frac{k_i}{m_i} & -\frac{\xi}{m_i} - \frac{c}{m_i} C_{L\alpha} \cos\beta_i \frac{q_\infty}{U} \end{bmatrix}, \qquad B_i(U, z_i) = \begin{bmatrix} 0 & 0 \\ \frac{p q_\infty c}{2 m_i s} & 0 \end{bmatrix}, \tag{68}$$

and mistuning can appear as $k_i = k_0(1 + z_i)$, $m_i = m_0(1 + z_i)$ or $\beta_i = \beta_0(1 + z_i)$. Notice that $M(U, z)$ is independent of the equilibrium vector $[\sigma_1, \ldots, \sigma_r]$ because the quasi-steady model is *linear*.

If we consider more general models, $M(U, 0)$ will still be of block circular structure as in (67). Here, the A matrices along the diagonal reflect forces on blades due to their own motion, while B is a coupling term between adjacent blades. In this case coupling of the upper blade enters as B while the lower blade generates a symmetric force of $-B$. More generally, we can have $B_{up} \neq -B_{down}$, and coupling between blades two, three or four apart would appear as C_{up}, C_{down}, D_{up}, D_{down}, E_{up}, E_{down}, and so forth. Size of $M(U, z)$ will be states per blade m, times number of blades r, for a total of $m \times r$. The circular structure of $M(U, 0)$ in equation (67) is a result of the circumferential symmetry of the problem and will be present for *any* discrete blade model.

B Eigenvalues and Eigenvectors of Block Circular Matrices

Motivated by Appendix A we consider block circular matrices and derive some standard results. Let $P \in \mathbb{R}^{\mathrm{rm} \times \mathrm{rm}}$ be defined as

$$P = \begin{bmatrix} P_1 & P_2 & P_3 & \ldots & P_{r-1} & P_r \\ P_r & P_1 & P_2 & P_3 & \ldots & P_{r-1} \\ & \ddots & & \ddots & & \\ & & \ddots & & \ddots & \\ P_2 & P_3 & \ldots & P_{r-1} & P_r & P_1 \end{bmatrix}, \tag{69}$$

where $P_j \in \mathbb{R}^{m\times m}$ for all j. Denote powers of the rth root of unity as $p_j = \exp(2\pi ij/r)$, here $i = \sqrt{-1}$. Now let

$$Q_j = P_1 + p_j P_2 + p_j^2 P_3 + \cdots + p_j^{r-1} P_r \in \mathbb{C}^{m\times m}, \quad j \in (1, 2, \ldots, r). \tag{70}$$

The following theorem allows us to express the eigenvalues and vectors of P as eigenvalues and vectors of Q_j's. Consequently, instead of solving the $rm \times rm$ eigenvalue/vector problem where computation time increases as $(rm)^3$, we can solve an $m \times m$ eigenvalue/vector problem r times with resulting computation time rm^3, a savings of r^2.

Theorem B.1 *For P a block circular matrix as above, let λ_j^d, u_j^d and v_j^d be the dth eigenvalue, left eigenvector and right eigenvector, respectively, of Q_j. Then λ_j^d form the eigenvalues of P with left and right eigenvectors $U_j^d = [u_j^d, p_j^{r-1}u_j^d, p_j^{r-2}u_j^d, \ldots, p_j u_j^d]$ and $V_j^d = [v_j^{d\prime}, p_j v_j^{d\prime}, \ldots, p_j^{r-2}v_j^{d\prime}, p_j^{r-1}v_j^{d\prime}]'$.*

Proof: To prove the theorem we need only show $PV_j^d = \lambda_j^d V_j^d$ and $U_j^d P = \lambda_j^d U_j^d$. Both statements are verified trivially by substitution. □

It follows from the theorem that block circular matrices have distinct eigenvalues generically. This is trivial to see for the scalar block case ($m = 1$) since the eigenvalues are simply the Q_j's. Hence for non-distinct eigenvalues we must have $Q_i = Q_j$ for $i \neq j$ —an extra condition on the P_is which will not hold in general. For block circular matrices the same condition applies, $Q_i = Q_j$ for $i \neq j$ implies non-distinct eigenvalues. However, in the latter case we can have non-distinct eigenvalues when a particular Q_j has non-distinct eigenvalues or if an eigenvalue of Q_j equals an eigenvalue of Q_i for $Q_i \neq Q_j$. Both additional cases are also degenerate and hence circular matrices have distinct eigenvalues generically. In other words, if we generate block circulant matrices at random then the set of matrices with non-distinct eigenvalues forms a measure zero set.

However, models are not generated at random and some common model structures lead to degenerate matrices. For example, if we have a model with no blade coupling then the resulting degenerate circular Jacobian would have the form $P_1 \neq 0$ and $P_2 = P_3 = \cdots = P_r = 0$ in which case $Q_1 = Q_2 = \cdots = Q_r = P_1$ and all the eigenvalues are non-distinct. Another example is the quasi-steady model used in Appendix A. This model is degenerate because it only includes coupling between adjacent blades and so $P_1 \neq 0, -P_2 = P_r \neq 0$ while $P_3 = P_4 = \cdots = P_{r-1} = 0$. Hence some of the Q_j's repeat and there are some non-distinct eigenvalues. It is important to realize that in these cases the non-distinct eigenvalues are generically simple (have diagonal Jordan form) and so travel smoothly with parameters. This is because each of the Q_j's will have distinct eigenvalues generically. As a result, each Q_j will typically have a complete set of left and right eigenvectors $\{u_j^d, v_j^d\}_{d=1}^m$ and so P will have a complete set of left and right eigenvector $\{U_j^d, V_j^d\}_{j,d=1}^{r,m}$. Notice that unlike the block matrices Q_j, the eigenvectors U_j^d, V_j^d will not repeat. So in the case where Q_j's repeat we will have non-distinct but typically simple eigenvalues which travel smoothly with parameters. If it so happens that the least stable eigenvalue is one of the non-distinct eigenvalues then the only analysis extension required is to keep track of multiple eigenvalues.

In the final degenerate case where one of the Q_j's is non-simple the eigenvalues may travel discontinuously with parameters, here the analysis fails and cannot be easily extended. We do not expect to encounter this case in practice because it is a measure zero set and there is no expected model structure that would enforce a non-simple Q_j.

To conclude this section we state a technical lemma required in Section 4 whose proof follows easily from properties of symmetric matrices and is not shown.

Lemma B.1 *If $R \in \mathbb{R}^{n\times n}$ is a real symmetric matrix, Γ is any open neighbourhood in $\mathbb{R}^n$ about the origin, then $z'Rz = 0, \forall z \in \Gamma$ if and only if $R = 0$.*

References

[1] F.A. Al-Khayyal, C. Larsen, and T. Van Voorhis. "A relaxation method for nonconvex quadratically constrained quadratic programs". *Journal of Global Optimization*, 6,no.3:215–230, 1995.

[2] O.O. Bendiksen. "Flutter of mistuned turbomachinery rotors". *ASME Journal of Engineering for Gas Turbines & Power*, 106:25–33, 1984.

[3] O.O. Bendiksen. "Recent developments in flutter suppression techniques for turbomachinery rotors". *J.Propulsion*, 4,no.2:164–171, 1986.

[4] H. Bloemhof. "Flutter of mistuned cascades with structural coupling". In *Unsteady Aerodynamics & Aeroelasticity of Turbomachines & Propellers*, 1987.

[5] E.F. Crawley and K.C. Hall. "Optimization and mechanisms of mistuning in cascades". *ASME 84-GT-196*, 1984.

[6] J. Dugundji and D.J. Bundas. "Flutter and forced response of mistuned rotors using standing wave analysis". *AIAA Journal*, 22,no.11:1652–61, 1984.

[7] R.C.F. Dye and T.A. Henry. "Vibration amplitudes of compressor blades resulting from scatter in blade natural frequencies". *ASME Journal of Engineering for Power*, 91:182–188, July 1969.

[8] L.E. El-Bayoumy and A.V. Srinivasan. "Influence of mistuning on rotor-blade vibrations". *AIAA Journal*, 13:460–464, April 1975.

[9] E. M. Greitzer. "The stability of pumping systems—the 1980 freeman scholar lecture". *ASME Journal of Fluids Engineering*, 103:193–242, 1981.

[10] K.R. Kaza and R.E. Kielb. "Flutter and response of a mistuned cascade in incompressible flow". *AIAA Journal*, 20:1120–1127, Aug 1982.

[11] D.E. Knuth. *Sorting and Searching*, volume 3 of *The Art of Computer Programming*. Addison-Wesley, 1973.

[12] P. Lancaster. "On eigenvalues of matrices dependent on a parameter". *Numerische Mathematik*, 6:377–387, 1964.

[13] K.G. Murty and S.N. Kabadi. "Some NP-complete problems in quadratic and nonlinear programming". *Mathematical Programming*, 39:117–129, 1987.

[14] E. Nissim and R.T. Haftka. "Optimization of cascade blade mistuning, part II: Global optimum & numerical optimization". *AIAA Journal*, 23,no.9:1402–10, 1985.

[15] C. Pierre and E.H. Dowell. "Localization of vibrations by structural irregularity". *Journal of Sound & Vibrations*, 114,no.3:549–64, 1987.

[16] C. Pierre and D.V. Murthy. "Aeroelastic modal characteristics of mistuned blade assemblies: Mode localization and loss of eigenstructure". *AIAA Journal*, 30,no.10:2483–96, 1992.

[17] A.V. Srinivasan and H.M. Frye. "Effects of mistuning on resonant stresses of turbine blades". In *Structural Dynamic Aspects of Bladed Disk Assemblies*, 1976.

[18] D.S. Whitehead. "Force and moment coefficients for vibrating airfoils in cascade". *Great Britian A.R.C.*, R. & M. 3254, 1960.

[19] D.S. Whitehead. "Torsional flutter of unstalled cascade blades at zero deflection". *Great Britian A.R.C.*, R&M 3429, 1964.

[20] D.S. Whitehead. "Effect of mistuning on the vibration of turbomachine blades induced by wakes". *Journal of Mechanical Engineering Science*, 8:15–21, March 1966.